

# The effect of crystallinity on fracture and yielding of polyethylenes

X. Lu, R. Qian and N. Brown\*

Department of Materials Science and Engineering, University of Pennsylvania, Philadelphia, PA 19104-6272, USA

(Received 20 April 1995)

The effect of the amount of crystallinity on fracture and yielding of polyethylenes as a function of temperature is reviewed. In particular, the effect of fracture toughness,  $K_c$ , at low temperatures is investigated. Generally,  $K_c$  increased linearly as density decreased. However, it was found that very low-density polyethylene shows a significant decrease in  $K_c$  from this general behaviour.

(Keywords: polyethylenes; crystallinity; failure modes)

## INTRODUCTION

The amount of crystallinity ( $X$ ) has a profound effect on the fracture and yielding of polyethylenes (PE). However, the influence of  $X$  depends on the temperature of deformation. In the temperature range where yielding is the failure mode, the yield point increases with  $X$ . In the low-temperature regime, where brittle fracture is the failure mode, the fracture toughness ( $K_c$ ) generally increases as  $X$  decreases for linear polyethylenes, but low-density polyethylenes with long branches (LDPE) are much less tough. In the case of failure by slow crack growth,  $X$  is not the primary factor in determining the time to failure. Branch density and placement of branches with respect to the molecular-weight distribution are most important as reported by Brown *et al.*<sup>1</sup>

In this paper the effect of  $X$  on fracture and yielding of PE as a function of temperature will be reviewed, and in particular the effect of  $K_c$  at low temperatures will be explored in greater detail.

There have been extensive investigations of the effect of  $X$  on the yield point, ( $\sigma_y$ ) at room temperature, as reported by Popli and Mandelkern<sup>2</sup>, Williamson *et al.*<sup>3</sup> and Fleissner<sup>4</sup>. There is general agreement that  $\sigma_y$  is nearly a linear function of  $X$  and that this relationship is rather insensitive to the conditions of crystallization. Crist *et al.*<sup>5</sup> have pointed out that the yield point increases with lamella thickness. It is not a simple matter to separate the effect of  $X$  and lamella thickness because usually lamella thicknesses increase with  $X$ .

The effect of morphology and molecular structure on low-temperature brittle fracture have been investigated by Chan and Williams<sup>6</sup>, Mandell *et al.*<sup>7</sup>, Brown and Ward<sup>8</sup> and Mirabella *et al.*<sup>9</sup>. Their results showed that  $K_c$  increased as  $X$  decreased. In particular, Mirabella *et al.*<sup>9</sup> attributed the toughness of linear low-density PE to the presence of rubber particles, which form at high branch

densities. Brown and Ward<sup>8</sup> related the low-temperature brittle fracture stress to the number of tie molecules. In this investigation  $K_c$  was measured over a very wide range of densities. Generally,  $K_c$  increased linearly as density decreased. However, very low-density PE shows a significant decrease in  $K_c$  from this general behaviour.

## EXPERIMENTAL

The PE resins were a variety of commercial resins with densities from 914 to 971 kg m<sup>-3</sup>. Most of the resins were linear copolymers with short branch densities ranging from 0 to 20 per 1000 carbon atoms and different types of short chain branches as shown in Table 1 with  $M_w$  generally in the range of 10<sup>5</sup> to 3 × 10<sup>5</sup>. Two long branched low-density homopolymers (LDPE) were also tested. Most specimens were compression moulded into 4.5 mm thick plaques and slow cooled. A few specimens were taken from pipe and some were rapidly quenched after compression moulding.

The yield points were measured at room temperature at a strain rate of 0.3 min<sup>-1</sup>. The low-temperature fracture stress was measured on notched specimens with a 4.5 × 4.5 mm<sup>2</sup> cross-section and a 15 mm gauge length. A 0.40 mm deep notch was made by slowly pressing a razor blade into the specimen. The test was conducted by immersing the specimen in liquid nitrogen (LN) for 20 min and quickly loading the specimen on a 20:1 ratio lever loading machine with a fixed load. The time to failure was recorded. Failure times ranged from 10<sup>3</sup> to 10<sup>-1</sup> min depending on the load.

## RESULTS

Figure 1 shows the  $\sigma_y$  versus density plot at room temperature. It should be noted that the resins with carbon black have a density that is about 5 kg m<sup>-3</sup> greater than for the unpigmented resin. The data in Figure 1 agree with previous investigations<sup>2-4</sup>.

\* To whom correspondence should be addressed

**Table 1** Physical and molecular parameters of PE resins

Resin No.	Density (g cm <sup>-3</sup> )	Yield stress (MPa)	Molecular parameters <sup>a</sup>
1	0.9476	20.4	E-H, 3.6 butyl branches/1000C, Mfr. 1970
2	0.9445	19.6	E-H, 4.9 butyl branches/1000C, $M_n = 15\,000$ , $M_w = 170\,000$ , Mfr. 1985
3	0.9435	19.6	E-H, 4.5 butyl branches/1000C, $M_n = 5300$ , $M_w = 170\,000$ , $MI = 0.19$ , NBS = GRI resin
4	0.9440	19.6	E-H, 4.8 butyl branches/1000C, $M_n = 12\,000$ , $M_w = 192\,000$ , $M_z = 1\,096\,000$ , $MI = 0.1$ , Mfr 1988
5	0.9452	19.9	E-H, unpigmented, 4.5 butyl branches/1000C
6	0.9430	19.4	E-H, $MI = 0.2$ , 4.5 butyl branches/1000C
7	0.9450	20.1	E-H, $MI = 0.13$ , 4.5 butyl branches/1000C
8	0.9481	21.4	E-H, 2.4% hexene by weight, $M_n = 11\,017$ , $M_w = 180\,000$ , $MI = 0.2$ , Mfr. 1988
9	0.9451	20.3	E-H, $MI = 0.16$ , Mfr. 1988
10	0.9451	20.2	E-H, $MI = 0.13$ , Mfr. 1988
11	0.9465	19.6	E-H, 4 butyl branches/1000C, $M_n = 20\,800$ , $M_w = 180\,277$ , $MI = 0.2$ , Mfr. 1988
12	0.9554	20.4	E-H
13	0.9515	19.9	E-H, Mfr. 1988
15	0.9512	22.6	E-H, 2.6 butyl branches/1000C, $M_w = 290\,000$
16	0.9472	20.5	E-4M, green pigment
17	0.9513	19.4	E-H
18	0.9552	20.9	E-B
19	0.9514	18.8	E-H
20	0.9710	27.6	E-B
21	0.9556	21.5	E-B, unpigmented resin, Mfr. 1986
22	0.9580	21.8	E-B
23	0.9629	24.6	E-B
24	0.9536	24.7	E-B
25	0.9552	24.3	E-B, 3.2 ethyl branches/1000C, $M_n = 10\,000$ , $M_w = 267\,000$ , $M_z = 2\,043\,000$ , Mfr. 1988
26	0.9574	25.4	E-B, $M_n = 14\,530$ , $M_w = 429\,416$ , $M_z = 6\,684\,586$
27	0.9560	25.7	E-B, $MI = 0.05$ , $M_n = 15\,000$ , $M_w = 200\,000$
28	0.9454	18.7	E-B, 3.6% butene by weight, $MI = 0.236$ , $M_n = 11\,200$ , $M_w = 150\,000$
29	0.9432	20.0	E-O, 4.5 hexyl branches/1000C, $MI = 1.0$ , unpigmented resin
30	0.9400	18.4	E-O, 5.8 hexyl branches/1000C, $MI = 3.0$ , unpigmented resin
31	0.9490	18.6	E-B, 2306I, brown pigment, Mfr. 1970
32	0.9465	20.7	E-O, 4.5 hexyl branches/1000C, $MI = 1.0$ , Mfr. 1987
33	0.9715	30.58	linear polymer, $M_n = 19\,600$ , $M_w = 130\,000$
34	0.9147		E-H, 20 butyl branches/1000C, $MI = 0.27$
35	0.9345		LDPE homopolymer, 7–8/1000C C <sub>2</sub> –C <sub>4</sub> branches and ≈3/1000C long branches, $MI = 1.6$ , $M_w = 78\,000$ , $M_n = 22\,000$
36	0.9243		LDPE homopolymer 12/1000C short branches C <sub>2</sub> –C <sub>4</sub> and 3/1000C long branches C <sub>6</sub> –C <sub>n</sub> , $M_w = 80\,000$ , $M_n = 23\,000$ , $MI = 2.3$

<sup>a</sup> E-H, ethylene–hexene; E-4M, ethylene–4-methylpentene; E-B, ethylene–butene; E-O, ethylene–octene copolymers. Mfr., year manufactured

Fleissner's<sup>4</sup> results on 32 PE resins are included in *Figure 1*. The physical basis for *Figure 1* is straight-forward. At room temperature, which is above  $T_g$ , the amorphous region has practically no resistance to shear compared to the crystalline region.

*Figure 2* shows time to fracture in LN versus the stress. As shown previously by Kamei and Brown<sup>10</sup>, the LN enhances crazing in PE as it does in all polymers. The LN acts as an environmental stress cracking agent. The slopes of the curves in *Figure 2* are about the same for all PE, but the shift along the stress axis is related to the density of the PE. *Figure 3* shows the fracture stress ( $\sigma_f$ ) versus density, where  $\sigma_f$  was measured for loading times less than about 30 s. All the points in *Figure 3* are for linear PE except for points 35 and 36, which are for LDPE. Generally, the density decreases as the density of short chain branches increases. The short chain branch density varies from 0 to about 5 branches for all the linear resins except for point 34, which has about 20 branches/1000C. The irregular points 34, 35 and 36 are the results of more extensive testing consisting of 10 tests each with standard deviations of 6, 12 and 6% respectively. The difference between the quenched and slow cooled state was measured for five resins. The results are shown in *Table 2*. For the quenched state  $\sigma_f$  is always greater than for the slow cooled state. It should also be observed that the change in density as produced by quenching increases with the density.

## DISCUSSION

At room temperature  $\sigma_y$  increases linearly with  $X$  as shown in *Figure 1* because the yield strength of the amorphous region is small compared to that of the crystalline region. However, as the temperature is raised above room temperature,  $\sigma_y$  of the crystalline region decreases to zero at a temperature corresponding to the melting point of the lamella crystal. In general, the melting point increases with the lamella thickness, and usually higher crystallinities are associated with thicker lamellae. As a result,  $\sigma_y$  becomes zero at a melting-point temperature that increases with  $X$  as shown in *Figure 4*.

When the temperature is decreased below room temperature, the effect of crystallinity on  $\sigma_y$  approaches zero at about 150 K as shown in *Figure 4*. This means that at 150 K the yield point of the amorphous region is equal to that of the crystalline region. *Figure 4* indicates that the differences in  $\sigma_y$  as caused by differences in  $X$  are greatest in the temperature range of 225–250 K.

It is interesting to compare the effects of  $X$  and temperature on  $\sigma_y$  with their effects on Young's modulus  $E$ . *Figure 5* shows that the difference in  $E$  with respect to a difference in  $X$  is approximately independent of temperature. Thus, the curves in *Figure 5* can be described in the temperature range 78–300 K by:

$$E = f_E(T) + DX \quad (1)$$

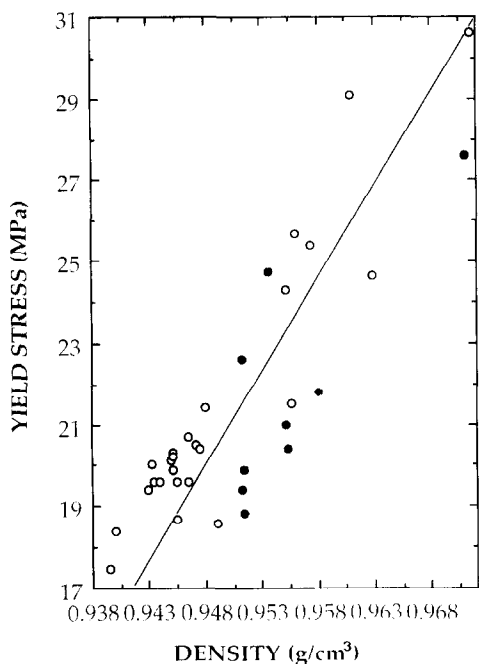


**Figure 1** Yield point versus density at room temperature and strain rate  $0.3 \text{ min}^{-1}$  for a variety of linear commercial PE resins. The straight line is from data by Fleissner<sup>4</sup>

where  $D$  is independent of  $T$  and  $f_E(T)$  is independent of  $X$ . If  $X = 0, f_E(T) = f_a(T)$ , where  $f_a(T)$  is the temperature dependence of  $E$  for the non-crystalline region. This result suggests that most of the change in  $E$  from 78 to 300 K is associated with the non-crystalline region (i.e. amorphous plus fringe region of crystals).

The dependence of  $\sigma_y$  on  $X$  and  $T$  is more complex in that:

$$\sigma_y = f_y(X, T) \quad (2)$$

However,  $E$  and  $\sigma_y$  are approximately proportional at all temperatures, as shown by Figure 6.

Brown<sup>11</sup> has proposed that the yield point of all polymers is proportional to the shear modulus below  $T_g$ . In the temperature range of about 125–300 K for PE, the ratio of  $\sigma_y/E$  varies from 0.016 to 0.029. Data gathered by Brown give an average value of  $\tau_y/G(0 \text{ K}) = 0.076 \pm 0.03$  for 12 amorphous polymers, where  $\tau_y$  is the shear yield point and  $G$  is shear modulus. When the data in Figures 4 and 5 are extrapolated to 0 K,  $\tau_y/G(0 \text{ K}) = 0.02$ . It is expected that  $\tau_y/G(0 \text{ K})$  for PE should be less than that for amorphous polymers, because the yield point in a crystalline solid is expected to be less than in an amorphous solid far below  $T_g$  because dislocations exist in crystals and because  $G(K)$  for a

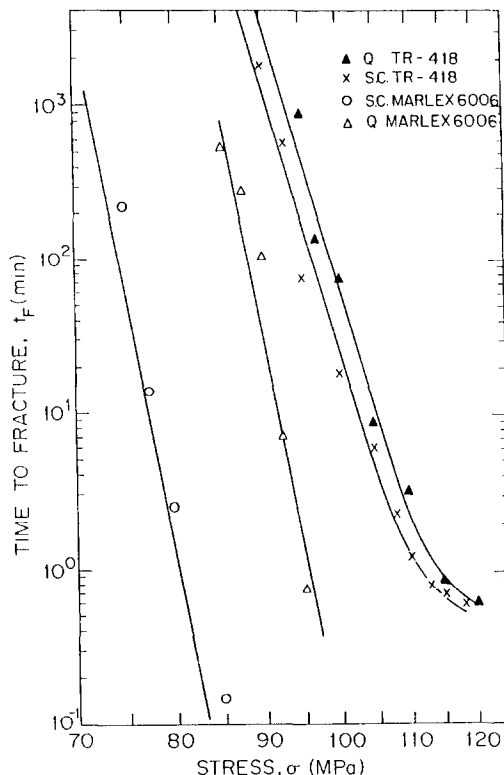


**Figure 2** Time to fracture in liquid nitrogen versus stress on specimens with 0.40 mm notch

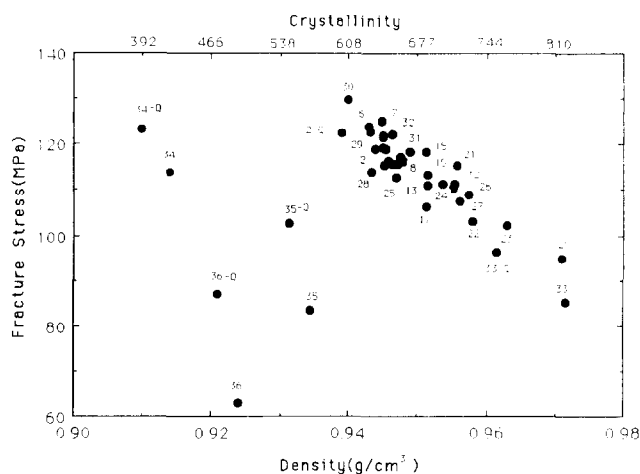


**Figure 3** Fracture stress for times less than 30 s in liquid nitrogen versus density of resins in Table 1

**Table 2** Effect of quenching on density and fracture stress

Material	Density ( $\text{kg m}^{-3}$ )		$\Delta\rho$ ( $\text{kg m}^{-3}$ )	$\sigma_f$ (MPa)	
	Quenched	Slow cooled		Quenched	Slow cooled
Homopolymer	961.0	971.5	105	98	85
4.5 butyl/1000C	939.5	945.5	60	128	119
7/1000C short branches and 3/1000C long branches	931.5	934.5	30	103	83
12/1000C short branches and 3/1000C long branches	922.3	924.3	20	88	63
20 butyl/1000C	912.8	914.7	19	120	114

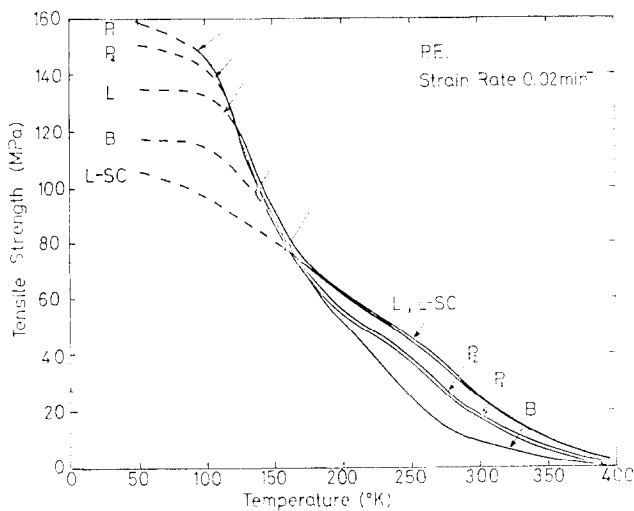


**Figure 4** Ultimate stress *versus* temperature. Full curves, yield point; broken curves, brittle fracture stress. L and L-SC are linear homopolymers. P<sub>1</sub> and P<sub>2</sub> are linear copolymers and B is a LDPE

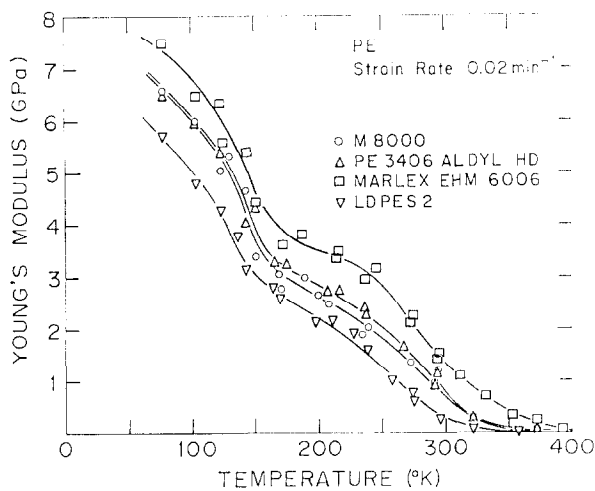


**Figure 5** Young's modulus *versus* temperature for various PE

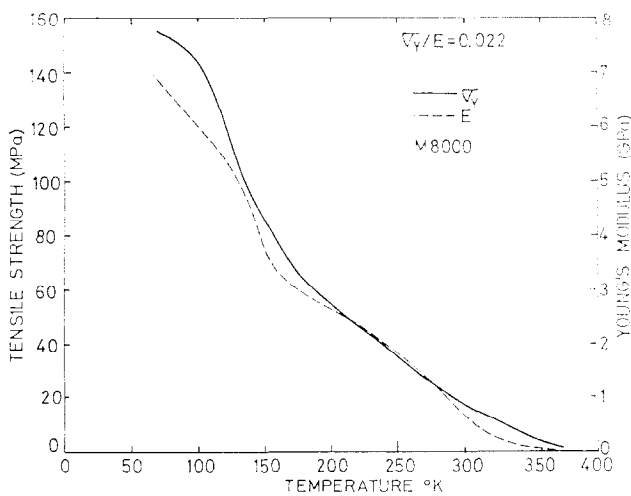


**Figure 6** Yield point and Young's modulus *versus* temperature for a copolymer

crystal should be greater than that for the amorphous state.

The low-temperature brittle fracture will now be discussed in terms of the fracture toughness:

$$K_{Ic} = Y\sigma_f\sqrt{a} \quad (3)$$

$Y = 2.1$  for the single edge-notched specimen and  $a = 0.40$  mm; therefore,  $K_{Ic} = 0.042\sigma_f \text{ MPa m}^{1/2}$ . The values of  $K_{Ic}$  for all the PE in this investigation range from 2.7 to 5.5  $\text{MPa m}^{1/2}$ .  $K_{Ic}$  from *Figure 3* appears to go through a maximum value between a density of 0.91 and 0.94  $\text{g cm}^{-3}$ . The behaviour of LDPE is anomalous relative to the behaviour of linear PE, being much weaker for a comparable density.

It is interesting to convert  $K_{Ic}$  to  $J_{Ic}$ , the  $J$  integral, which is related to the fracture energy. For the case of plane strain:

$$J_{Ic} = \frac{K_{Ic}^2}{E}(1 - \gamma^2) \quad (4)$$

The values of Young's modulus  $E$  range from about 5.5 to 7.5 GPa, and Poisson's ratio  $\gamma = 0.35$ . Thus, the values of  $J_{Ic}$  range from 1.2 to 4.8  $\text{kJ m}^{-2}$ . These values of fracture energy indicate that extensive deformation occurs in a thin layer of the fractured surface. Microscopic examination indicates that crazing precedes fracture. Kamei and Brown<sup>10</sup> have shown that LN enhances crazing. However, the differences in the fracture stress among the resins are attributed to differences in morphology. As indicated by *Figure 2*, the effect of LN is time-dependent as related to the slope of  $\sigma_f$  *versus* time, but the effect of molecular and morphological structure is associated with the horizontal shift of these curves relative to each other.

Microscopic observations (*Figure 7*) show that the roughness of the fractured surface increases with  $J_{Ic}$ . Since the degree of surface roughness is indicative of the fracture energy, the correlation of  $J_{Ic}$  and surface roughness is obvious. Mandell *et al.*<sup>7</sup> found the same results. A visual aid is presented to show how the fracture energy is related to density. *Figure 8* is a schematic of the microstructure of linear PE with different densities. The basic structure is a network of crystals and tie molecules. When a tensile stress is applied to this network, the tie molecules pull on the crystals and the crystals are unravelled. Finally, fracture occurs in the fibrils of a craze. The major part of the fracture energy is associated with the amount of plastic deformation that occurs when the crystals are unravelled during the production of the fibrils. Only a small amount of energy is required to fracture the covalent and van der Waals bonds. Thus, the amount of crystal deformation depends on the volume of crystals and the number of tie molecules that unravel the crystals. *Figure 8a* shows a homopolymer with a high crystallinity but only a few tie molecules whose fracture energy is low because the number of tie molecules is low. As the crystallinity is decreased the crystal size decreases and consequently the number of tie molecules increases. The probability of forming a tie molecule varies inversely with the long period as described by Huang and Brown<sup>12</sup>. Thus, the amount of deformation of the crystals is greater in *Figure 8b* than in *Figure 8a*. When the density becomes very low, the volume of crystals decreases. However, the number of tie molecules may not

change significantly as shown in Figure 8c because the long period may not change appreciably even though the lamella thickness is less. This schematic model indicates that the fracture energy is related to the product of the tie molecules and the crystallinity as follows:

$$K_{Ic} = C(tX) + B \quad (5)$$

where  $t$  is the density of tie molecules. The value of  $B$  can be obtained from Figure 3 when the data are extra-

polated to  $X=1$  where  $t$  is expected to go to zero. Thus,  $B = 1.5 \text{ MPa m}^{1/2}$ ;  $C$  is a constant to make the units consistent. An important aspect of equation (5) is that it goes through a maximum value as suggested by the data in Figure 3.

The low fracture toughness of the LDPE indicates that fewer tie molecules form as compared to the linear PE. For example, point 34 in Figure 3 is associated with a linear PE whose crystallinity is 16% less than that of the LDPE (point 35) and yet its  $K_{Ic}$  value is 39% greater. According to equation (5), this result indicates that the  $t$  for the linear PE is 2.4 times that for the LDPE. The reason for this difference is associated with the fact that the linear PE has a  $M_w$  of about 150 000 and the LDPE has a  $M_w$  of 78 000. The higher-molecular-weight molecule has a greater probability of forming a tie molecule. The LDPE has about three long branches/1000C. Thus, the distance between the ends of the molecule will be reduced relative to the end-to-end distance of a linear PE with the same  $M_w$ . Thus, the probability of forming a tie molecule is reduced. The range of motion of the free ends in the LDPE is restricted by the nodal points where the long branches join the main chain. This restricted motion would also reduce the probability of forming a tie molecule.

Generally, quenching reduces  $X$  and increases  $t$ . The density of tie molecules  $t$  increases as the long period decreases and  $t$  also increases because quenching changes the kinetics of crystallization so that a given molecule has less time to gather together into the same crystal. Crystallinity  $X$  decreases with quenching since less time is available to form crystals and the crystals tend to be thinner. It is interesting to note in Table 2 that the change in density produced by quenching decreases as the density of branches increases. The crystal thickness is governed by the distance between random entanglements and the distance between branches. As the density of branches increases, the effect of random entanglements on crystal thickness decreases. Since quenching can exert an influence on the spacing of random entanglements but not on the spacing of branches, the change in density from quenching decreases as the branch density increases. The increase in  $\sigma_f$  by quenching is caused by an increase in  $t$ , which is not offset by a concomitant decrease in  $X$ .

#### ACKNOWLEDGEMENTS

The research was supported by the Gas Research

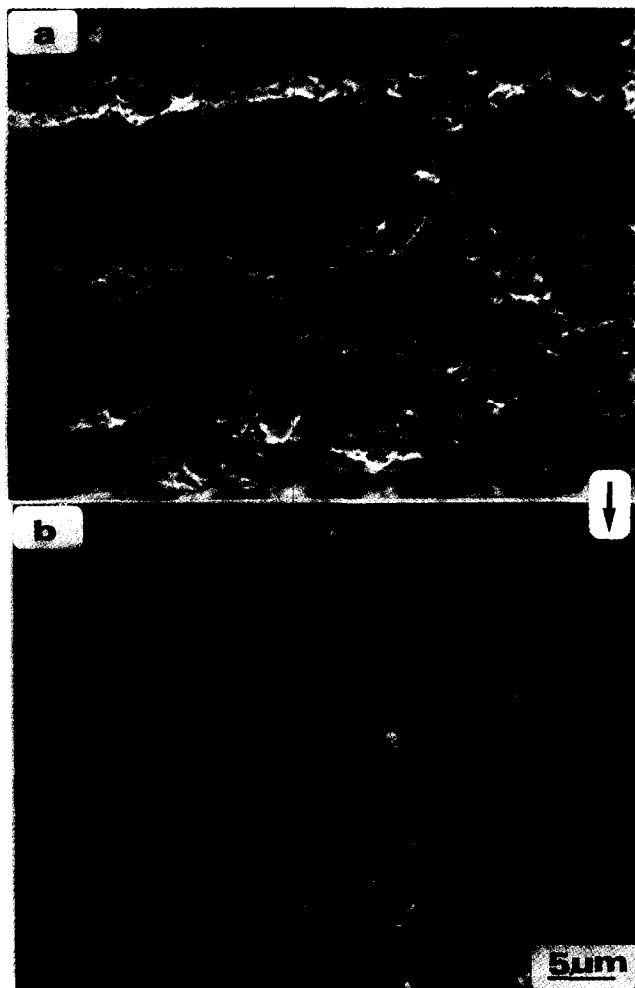


**Figure 7** Fractured surfaces of specimens fractured in liquid nitrogen: (a) is slow cooled ethylene-hexene resin,  $\sigma_f = 119 \text{ MPa}$ ; (b) is quenched state of same resin,  $\sigma_f = 128 \text{ MPa}$ . Note that the surface of the quenched specimen is much rougher than for slow cooled state. Arrow shows direction of crack propagation

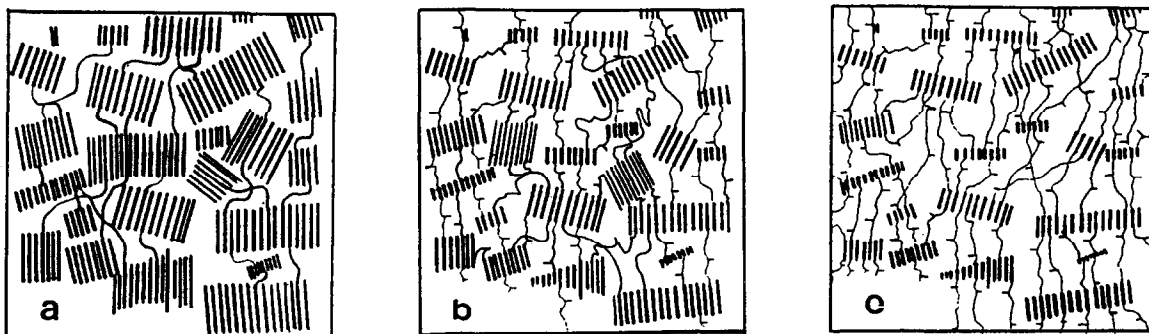


**Figure 8** Schematic of structure of linear PE: (a) high density, (b) medium density and (c) low density. White region between crystals is amorphous region. Lines between crystals are tie molecules

Institute. The Central Facilities of the Materials Research Laboratory as supported by the National Science Foundation under Grant No. DMR 91-20668 were most helpful.

#### REFERENCES

- 1 Brown, N., Lu, X., Huang, Y. and Qian, R. *Makromol. Chem.* 1991, **41**, 55
- 2 Popli, R. and Mandelkern, L. *J. Polym. Sci. Polym. Phys. Edn.* 1987, **25**, 441
- 3 Williamson, G. R., Wright, B. and Howard, J. *J. Appl. Chem.* 1964, **14**, 131
- 4 Fleissner, M. *Angew. Makromol. Chem.* 1982, **105**, 167
- 5 Crist, B., Fischer, C. J. and Howard, P. R. *Macromolecules* 1989, **22**, 1709
- 6 Chan, M. K. V. and Williams, J. G. *Polym. Eng. Sci.* 1990, **21**, 2007
- 7 Mandell, J. F., Roberts, D. R. and McGarry, F. J. *Polym. Eng. Sci.* 1983, **23**, 404
- 8 Brown, N. and Ward, I. M. *J. Mater. Sci.* 1983, **18**, 1405
- 9 Mirabella, F. M. Jr., Westphal, S. P., Fernando, P. L. and Ford, E. A. *J. Polym. Sci. (B) Polym. Phys.* 1988, **26**, 1995
- 10 Kamei, E. and Brown, N. *J. Polym. Sci., Polym. Phys. Edn.* 1984, **22**, 543
- 11 Brown, N. *J. Mater. Sci.* 1983, **18**, 2241
- 12 Huang, Y.-L. and Brown, N. *J. Polym. Sci., Polym. Phys. Edn.* 1990, **28**, 2007